

## Electrochemical Behaviour of AA6063 Alloy in Hydrochloric Acid using Schiff Base Compounds as Corrosion Inhibitors.

Sanaula Pathapalya Fakrudeen<sup>\*</sup>, Lokesh H. B<sup>\*\*</sup>, Ananda Murthy H. C<sup>\*\*\*</sup>,  
Bheema Raju V. B<sup>\*\*\*\*</sup>.

<sup>\*</sup>Department of Engineering Chemistry, HKBK College of Engineering, Nagawara, Bangalore Karnataka, India

<sup>\*\*</sup>Department of Engineering Chemistry, Vivekanand Institute of Technology, , Bangalore-Karnataka, India.

<sup>\*\*\*</sup>Department of Engineering Chemistry, R N Shetty Institute of Technology,  
Bangalore, Karnataka, India.

<sup>\*\*\*\*</sup>Department of Engineering Chemistry, Dr. Ambedkar Institute of Technology,, Bangalore , Karnataka, India.

### ABSTRACT

The electrochemical behavior of aluminium alloy AA6063 were investigated using Schiff base compounds namely N, N'-bis (Salicylidene)-1, 4-Diaminobutane (SDB) and N, N'-bis (3-Methoxy Salicylidene)-1, 4 Diaminobutane (MSDB) as corrosion inhibitors in presence of 1M Hydrochloric Acid by weight loss, Potentiodynamic polarization(PDP), electrochemical impedance spectroscopy(EIS) and scanning electron microcopy (SEM). Potentiodynamic polarization study revealed that the two Schiff bases acted as mixed type inhibitors. The change in EIS parameters is indicative of adsorption of Schiff bases on aluminum alloys surface leading to formation of protective layer. The weight loss study showed that the inhibition efficiency of these compounds increases with increase in concentration and vary with solution temperature and immersion time. The various thermodynamic parameters were also calculated to investigate the mechanism of corrosion inhibition. The effect of methoxy group on corrosion efficiency was observed from the results obtained between SDB and MSDB. The effectiveness of these inhibitors were in the order of MSDB>SDB. The adsorption of Schiff bases on AA6063 alloy surface in acid obeyed Langmuir adsorption isotherm. The surface characteristics of inhibited and uninhibited alloy samples were investigated by scanning electron microscopy (SEM).

**Keywords:** Electrochemical techniques, Corrosion, Schiff base, Adsorption, Aluminum alloy.

### 1. Introduction:

Corrosion of aluminum and its alloys has been a subject of numerous studies due to their high technological value and wide range of industrial applications especially in aerospace and house-hold industries. Aluminum and its alloys,

however, are reactive materials and are prone to corrosion. A strong adherent and continuous passive oxide film is developed on Al upon exposure to aqueous solutions. This surface film is amphoteric and dissolves when the metal is exposed to high concentrations of acids or bases [1]. Hydrochloric acid solutions are used for acid cleaning, acid de-scaling, chemical and electrochemical etching in many chemical process industries where in aluminium alloys are used. It is very important to add corrosion inhibitors to prevent metal dissolution and minimize acid consumption [2]. Most of the efficient acid inhibitors are organic compounds that contain mainly nitrogen, sulfur or oxygen atoms in their structure. The choice of inhibitor is based on two considerations: first it could be synthesized conveniently from relatively cheap raw materials; second, it contains the electron cloud on the aromatic ring or electronegative atoms such as nitrogen, oxygen in relatively long-chain compounds. Numerous organic substances containing polar functions with nitrogen, oxygen, and sulphur atoms and aromatic rings in a conjugated system have been reported as effective corrosion inhibitors for aluminium alloys [3-5]. Some Schiff bases have been reported earlier as corrosion inhibitors for aluminum alloys [6-8], iron [9-10] and copper [11-12]. Compounds with  $\pi$ -bonds also generally exhibit good inhibitive properties due to interaction of  $\pi$  orbital with metal surface. Schiff bases with  $RC = NR'$  as general formula have both the features combined with their structure which may then give rise to particularly potential inhibitors.

The present work is aimed at investigating the inhibitive ability of two Schiff base molecules on corrosion of AA6063 in 1M Hydrochloric acid medium. The weight loss, potentiodynamic polarization and electrochemical impedance techniques were employed to study inhibitive effect of two Schiff base molecules at different concentrations. The effect of temperature,

immersion time on corrosion behaviour of aluminium alloy was also studied in absence and presence of inhibitor at various concentrations. For further confirmation aluminum alloy samples were analyzed by scanning electron microscopic (SEM) technique.

The inhibition effect of Schiff base compounds are reported on steel [13-14], Copper [15], and pure aluminium and its alloys [16-19], in acidic medium. However, no substantial work has been carried out on corrosion inhibition of aluminium alloys in acidic medium by Schiff bases. Thus, it was thought worthwhile to study the corrosion inhibition effect of Schiff base compounds namely N, N'-bis (Salicylidene)-1, 4-Diaminobutane (SDB) and N, N'-bis (3-Methoxy Salicylidene)-1, 4 Diaminobutane (MSDB) on AA6063 Alloy in 1M Hydrochloric acid medium.

## 2. Experimental

### 2.1 Materials

The alloy samples were procured from M/S. Fenfe Metallurgical, Bangalore, India. The typical chemical composition of AA6063 alloy in weight percentage is shown in Table 1. The alloy

Table-1. Typical Chemical Composition of AA 6063

Element	Cu	Mg	Si	Fe	Mn	Ti	Cr	Zn	Others	Al
Wt.%	0.10	0.45 - 0.90	0.2 - 0.6	0.35 Max	0.10 Max	0.10 Max	0.10 Max	0.10 Max	0.15 Max	Reminder

### 2.2 Inhibitor.

The Schiff Bases were prepared by the condensation of respective aromatic aldehydes with each of diamines as per the reported procedure [20]. All reagents used were of analytical grade procured from Sigma Aldrich. N,N'-bis(Salicylidene)-1,4-Diaminobutane (SDB) was prepared by slow addition of Salicylaldehyde (2 mmol) in 30 mL methanol over a solution of 1,4-diaminobutane (1mmol) in 30 mL methanol and N,N'-bis(3-MethoxySalicylidene)-1,4-Diaminophenylene (MSDB) by slow addition of Methoxysalicylaldehyde (2 mmol) in 30 mL methanol over a solution of 1,4-diaminobutane (1 mmol) in 30 mL methanol taken in a 250 mL condensation flask. In each case, 2-3drops of acetic acid was added to the mixture of aldehyde and diamine with stirring at constant temperature 25°C for 1 hour. Further the mixture was refluxed for 4-5 hours on a water bath, heating occasionally to improve the yield of the product. The reaction mixture was cooled to room temperature overnight and the colored compound was filtered off and dried. The compounds were recrystallised with ethanol. The product identity was confirmed *via*

samples were cut into cylindrical test specimens and moulded in cold setting Acrylic resin exposing a surface area of 1.0 cm<sup>2</sup> for electrochemical measurements. For weight loss experiments the cylindrical alloy rods were cut into 24 mm dia x 2mm length -circular cylindrical disc specimens using an abrasive cutting wheel and a 2mm mounting hole at the centre of the specimen was drilled. Before each experiment, the electrodes were abraded with a sequence of emery papers of different grades (600, 800, and 1200), washed with double distilled water, degreased with acetone and dried at 353 K for 30 min in a thermostated electric oven and stored in a moisture-free desiccator prior to use. The corrosive medium selected for this study was 1M hydrochloric acid, which was prepared from analytical grade 37 percent acid concentrated (Merck ) in double distilled water.

melting points, Fourier transform infrared spectroscopy (FT-IR) and Proton Nuclear Magnetic Resonance (<sup>1</sup>H NMR). The structure, molecular formula, molecular mass, melting points are shown in Table-2.

N,N'-bis(Salicylidene)-1,4-Diaminobutane  
IR (KBr cm<sup>-1</sup>): 3400(OH), 3054(=C-H), 2903(-CH), 1628(C=N).

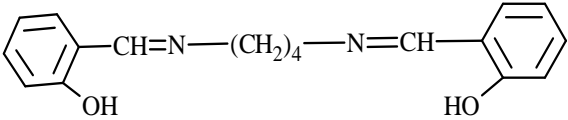
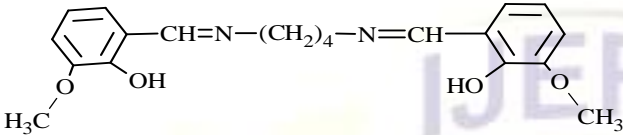
<sup>1</sup>HNMR (CDCl<sub>3</sub>): δ 1.79-1.82(t, 4H, -CH<sub>2</sub>CH<sub>2</sub>-), δ 3.62-3.65(t, 4H, -CH<sub>2</sub>-N) 6.84-7.31 (m, 8H, ArH). 8.34(s, 2H, N=CH), 13.49 (s, 1H, OH),

N,N'-bis(3-Methoxy Salicylidene)-1,4-Diaminobutane

IR (KBr cm<sup>-1</sup>): 3429(OH), 2996(=C-H), 2932(-CH), 1628(C=N). 1253(-OCH<sub>3</sub>).

<sup>1</sup>HNMR (CDCl<sub>3</sub>): δ 1.80-1.83(t, 4H, -CH<sub>2</sub>CH<sub>2</sub>-), δ 3.63-3.66(t, 4H, -CH<sub>2</sub>-N) δ 3.90(s, 6H, -OCH<sub>3</sub>), 6.77-7.2 (m, 6H, ArH). 8.32(s, 2H, N=CH), 14.00 (s, 1H, OH),

Table-2. The structure, molecular formula, molecular mass, melting points

Structure and Name	Molecular Formula	Molecular Mass	Melting Point
 <p>N,N'-bis(Salicylidene)-1,4-Diaminobutane (SDB)</p>	$C_{18}H_{20}N_2O_2$	296.36	89°C
 <p>N,N'-bis(3-Methoxy Salicylidene)-1,4-Diaminobutane (MSDB)</p>	$C_{20}H_{24}N_2O_4$	356.42	152°C

### 2.3 Weight loss measurements

Weight loss measurements were performed on aluminium alloys as per ASTM Method [21]. The test specimens were immersed in 100mL 1M hydrochloric acid solution in absence and presence of different concentrations (25,50,75 and 100 ppm) of SDB and MSDB at different temperature ranges (303, 313, 323 and 333 K) in thermostated water bath. The difference in weight for exposed period of 2, 4, 6 and 8 hours was taken as the total weight loss. The weight loss experiments were carried out in triplicate and average values were recorded. The corrosion rate was evaluated as per ASTM Method [21]. The percentage of inhibition efficiency ( $\mu_{WL}\%$ ) and the degree of surface coverage ( $\theta$ ) were calculated using equations (1) and (2):

$$\mu_{WL}\% = \frac{W_o - W_i}{W_o} \times 100 \quad (1)$$

$$\theta = \frac{W_o - W_i}{W_o} \quad (2)$$

Where  $W_i$  and  $W_o$  are the weight loss values of aluminium alloy sample in the presence and absence of the inhibitor and  $\theta$  is the degree of surface coverage of the inhibitor.

### 2.4 Electrochemical measurements.

Potentiodynamic polarization (PDP) and electrochemical impedance spectroscopy (EIS) measurements were performed using CH660c electrochemical work station. All electrochemical

experiments were measured after immersion of alloy specimens for 30 minutes to establish a steady state open circuit potential in absence and presence of inhibitors at 303 K.

Tafel plots were obtained using conventional three electrode Pyrex glass cell with alloy specimen ( $1\text{cm}^2$ ) as working electrode (WE), platinum electrode (Pt) as an auxiliary electrode and standard calomel electrode (SCE) as reference electrode. All the values of potential were referred to SCE. Tafel plots were obtained by polarizing the electrode potential automatically from  $-250$  to  $+250$  mV with respect to open circuit potential (OCP) at a scan rate  $1\text{mV s}^{-1}$ . The linear Tafel segments of anodic and cathodic curves were extrapolated to corrosion potential ( $E_{\text{corr}}$ ) to obtain corrosion current densities ( $I_{\text{corr}}$ ). The inhibition efficiency was evaluated from the  $I_{\text{corr}}$  values using the following relationship (3):

$$\mu_p\% = \frac{i_{\text{corr}}^0 - i_{\text{corr}}}{i_{\text{corr}}^0} \times 100 \quad (3)$$

Where,  $i_{\text{corr}}^0$  and  $i_{\text{corr}}$  are values of corrosion current densities in absence and presence of inhibitor respectively.

EIS measurements were carried out in a frequency range from 100 kHz to 0.01 Hz with small amplitude of 10mV peak -to-peak, using AC signal at OCP. The impedance data was analyzed using Nyquist plot and Echem software ZSimpWin version 3.21 was used for data fitting. The inhibition efficiency ( $R_{\text{ct}}\%$ ) was calculated from the charge transfer resistance ( $R_{\text{ct}}$ ) values using following equation (4):

$$\mu_{Ret} \% = \frac{R_{ct}^i - R_{ct}^0}{R_{ct}^i} \times 100 \quad (4)$$

Where,  $R_{ct}^0$  and  $R_{ct}^i$  are the charge transfer resistance in absence and presence of inhibitor, respectively.

### 2.5 Scanning electron microscopy (SEM).

The surface morphology of the corroded surface in the presence and absence of inhibitors were studied using scanning electron microscope (SEM) [Model No JSM-840A-JEOL]. To understand the morphology of the aluminium alloy surface in the absence and presence of inhibitors, the following cases were examined.

- (i) Polished aluminium alloy specimen.
- (ii) Aluminium alloy specimen dipped in 1M HCl.
- (iii) Aluminium alloy specimen dipped in 1M HCl containing 100 ppm of Schiff base.

## 3. Results and Discussion

### 3.1 Potentiodynamic polarisation (PDP)

The polarization measurements of AA6063 alloy specimens were carried out in 1M Hydrochloric acid, in the absence and in the presence of different concentrations (25 -100 ppm) of SDB and MSDB at 303K in order to study the anodic and cathodic reactions. The Fig.1(a) and (b). represents potentiodynamic polarisation curves (Tafel plots) of AA6063 alloy in 1M Hydrochloric acid in absence and presence of various concentrations of SDB and MSDB at 303K respectively. The electrochemical parameters i.e. corrosion potential ( $E_{corr}$ ), corrosion current density ( $i_{corr}$ ), cathodic and anodic Tafel slopes ( $b_a$  and  $b_c$ ) associated with the polarization measurements of SDB and MSDB are listed in Table.3. The inhibition efficiency ( $\mu_p$  %) of inhibitors at different concentrations was calculated from the equation (4). It is observed from the PDP results that, in presence of inhibitors, the curves are shifted to lower current density ( $i_{corr}$ ) regions and Tafel slopes  $b_a$  and  $b_c$  values increased with increase in concentration of inhibitors showing the inhibition tendency of SDB and MSDB. The corrosion potential ( $E_{corr}$ ) values do not show any appreciable shift, which suggest that both inhibitors acted as mixed type but predominantly cathodic inhibitors [22-23]. This can probably be due to the adsorption of protonated Schiff base molecules on the cathodic and anodic sites

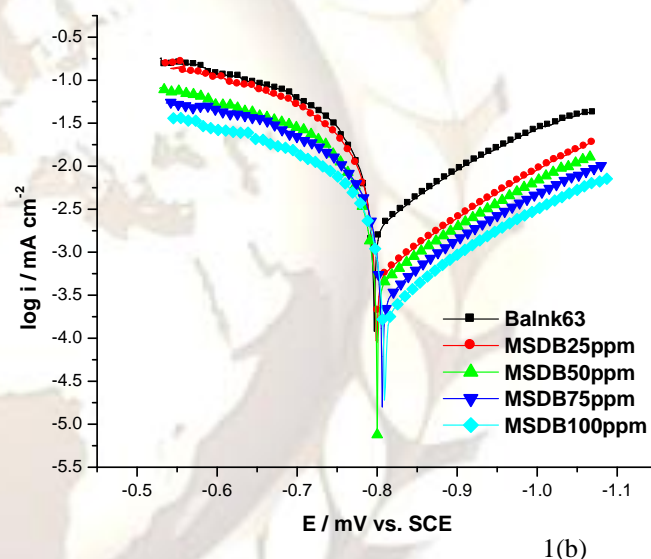
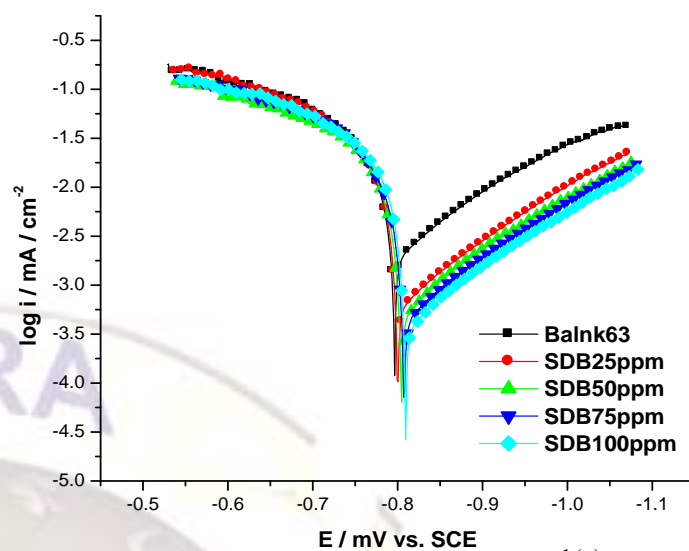


Figure. 1. potentiodynamic polarisation curves (Tafel plots) of AA6063 alloy in 1M Hydrochloric acid in absence and presence of various concentrations of (a) SDB and (b) MSDB at 303K

Table.3. Potentiodynamic polarisation parameters of AA6063 alloy in 1M Hydrochloric acid in absence and presence of various concentrations of SDB and MSDB at 303K

Inhibitor	Concentration (ppm)	$-E_{corr}$ (mV vs. SCE)	$i_{corr}$ ( $\text{mA cm}^{-2}$ )	$b_c$ ( $\text{mV dec}^{-1}$ )	$b_a$ ( $\text{mV dec}^{-1}$ )	$\mu_p$ %
SDB	0	797	3.29	187	47	---
	25	800	1.03	193	44	68.6
	50	804	0.95	195	50	71.1
	75	808	0.83	198	53	74.7
	100	810	0.68	203	55	79.3
MSDB	25	799	0.94	195	49	71.4
	50	801	0.79	199	50	75.8
	75	807	0.71	205	56	78.4
	100	809	0.61	214	66	81.4

### 3.2 Electrochemical impedance spectroscopy.

The effect of the inhibitor concentration on the impedance behavior of AA6063 alloy in 1M Hydrochloric acid was studied and Nyquist plots of AA6063 in absence and presence of various concentrations of Schiff bases are given in Fig 2 (a) and (b).

It is clear from the figure that the impedance diagrams obtained yield a semicircle shape. This indicates that the corrosion process is mainly controlled by charge transfer. The general shape of the Nyquist plots is similar for all samples of AA 6063 alloy, with a large capacitive loop at higher frequencies and inductive loop at lower frequencies. The similar impedance plots have been reported for the corrosion aluminum and its alloys in hydrochloric acid [24-30].

The Nyquist plot with a depressed semicircle with the center under the real axis is characteristic property of solid electrode and this kind of phenomenon is known as the dispersing effect [31-32]

An equivalent circuit fitting of five elements was used to simulate the measured impedance data of AA6063 alloy is depicted in Fig.3.

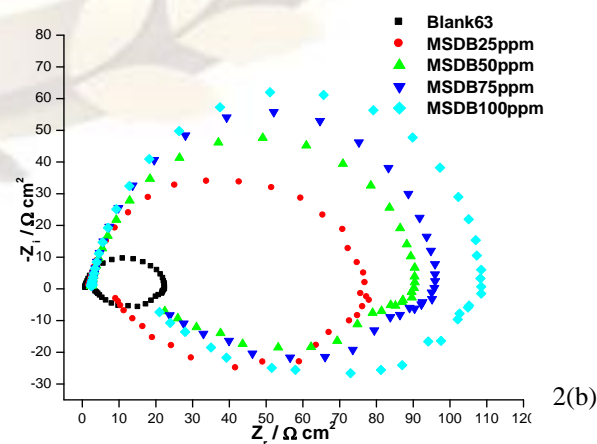
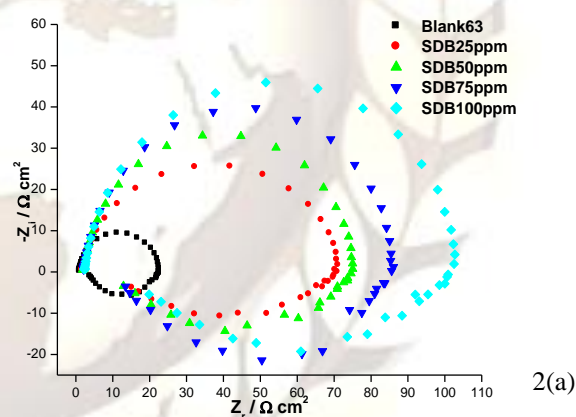


Figure. 2. Nyquist plot for AA6063 alloy in 1M Hydrochloric acid in absence and presence of various concentrations of (a) SDB and (b) MSDB at 303K

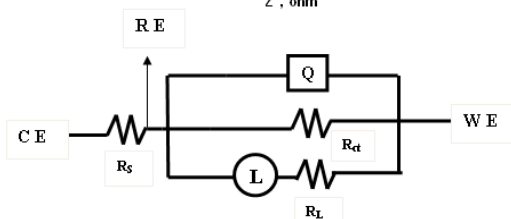
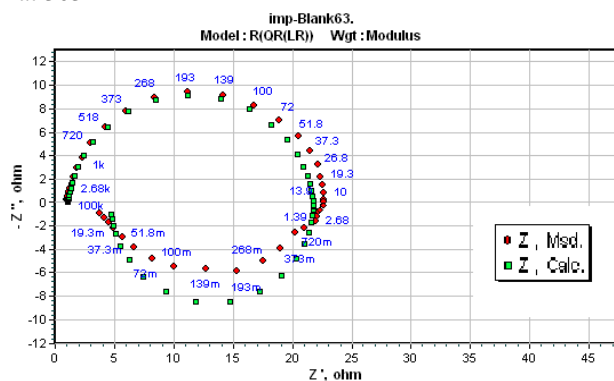


Figure.3. The equivalent circuit model used to fit the experimental impedance data.

The equivalent circuit includes solution resistance  $R_s$ , charge transfer resistance  $R_{ct}$ , inductive elements  $R_L$  and  $L$ . The circuit also consists of constant phase element, CPE ( $Q$ ) in parallel to the parallel resistors  $R_{ct}$  and  $R_L$ , and  $R_L$  is in series with the inductor  $L$ . The impedance spectra for the aluminium alloy in absence and presence of the inhibitors are depressed. The deviation of this kind is referred as frequency dispersion, and has been attributed to inhomogeneous of solid surface of aluminum alloy. Assumption of a simple  $R_{ct}-C_{dl}$  is usually a poor approximation especially for systems showing depressed semicircle behavior due to non-ideal capacitive behaviour of solid electrodes [33]. The capacitor in the equivalent circuit can be replaced by a constant phase element (CPE), which is a frequency dependent element and related to surface roughness. CPE is substituted for the respective capacitor of  $C_{dl}$  in order to give a more accurate fit. The impedance function of a CPE is defined in impedance [34] representation as (5).

$$Z_{CPE} = \frac{1}{(Y_0 j \omega)^n} \quad (5)$$

Where,  $Y_0$  magnitude of CPE,  $n$  is exponent of CPE, and are frequency independent, and  $\omega$  is the angular frequency for which  $-Z''$  reaches its maximum value,  $n$  is dependent on the surface morphology:  $-1 \leq n \leq 1$ .  $Y_0$  and  $n$  can be calculated by the equation proved by Mansfeld et al

[35]. The double layer capacitance ( $C_{dl}$ ) can be calculated from the equation.(6) [36].

$$C_{dl} = Y_0 (\omega_{max})^{n-1} \quad (6)$$

Where  $Y_0$  is the magnitude of the constant phase element and  $\omega_{max}$  is the angular frequency at which  $-Z''$  reaches maximum and  $n$  is the CPE exponent.

The electrochemical impedance parameters  $R_s$ ,  $R_{ct}$ ,  $\omega$ , CPE,  $n$  and  $C_{dl}$  are listed in Table-4.

The inhibition efficiency was evaluated by  $R_{ct}$  and  $C_{dl}$  values of the impedance data, it is shown from Table.(4) that charge transfer resistance ( $R_{ct}$ ) of inhibited system increased and double layer capacitance ( $C_{dl}$ ) decreased with increase in inhibitor concentration. This was due to adsorption of Schiff base molecule on the metal surface, the adsorbed inhibitor blocks either cathodic or anodic reaction or both formation of physical barrier, which reduces metal reactivity. The effect of inhibitor may be due to changes in electric double layer at the interface of solution and metal electrode. The decrease in double layer capacitance ( $C_{dl}$ ) can be caused by decrease in local dielectric constant and /or increase in the thickness of electric double layer, this suggest that the Schiff base molecules inhibit the aluminium alloy by adsorption at the metal – acid interface. It is evident that the inhibition efficiency increases with increase in inhibitor concentration which is in good agreement with the Potentiodynamic polarization results.

Table-4. Electrochemical impedance parameters of AA6063 alloy in 1M Hydrochloric acid in absence and presence of various concentrations of (a) SDB and (b) MSDB at 303K

Inhibitor	Concentration (ppm)	$R_s$ ( $\Omega \text{ cm}^{-2}$ )	$R_{ct}$ ( $\Omega \text{ cm}^{-2}$ )	$\omega$ (Hz)	CPE ( $\mu\text{F cm}^{-2}$ )	$n$	$C_{dl}$ ( $\mu\text{F cm}^{-2}$ )	$\mu_{R_{ct}}$ %
SDB	0	1.06	21	9.4	71.0	0.9225	52	---
	25	1.03	65	25.6	38.8	0.9091	24	67.7
	50	1.09	70	33.0	29.0	0.9101	18	70.0
	75	1.15	81	40.0	27.0	0.9147	17	74.3
	100	1.19	96	46.0	25.0	0.9260	16	78.0
MSDB	25	1.12	73	40.0	35.5	0.8831	20	71.6
	50	1.19	87	49.0	26.0	0.9098	16	75.8
	75	1.21	95	56.0	22.1	0.9118	13	77.9
	100	1.22	108	62.0	18.2	0.9158	11	80.5

### 3.3 Weight loss measurements

The experimental data of weight loss ( $\Delta w$ ), percentage of inhibition efficiency ( $\mu_{WL}\%$ ), Corrosion Rate (C.R.) in mmpy and degree of Surface Coverage ( $\theta$ ) for AA6063 in 1M Hydrochloric acid in absence and presence of various concentration of SDB and MSDB Schiff bases at 2 hours of exposure time and different temperature are shown in Table. 5.

#### 3.3.1 Effect of inhibitor concentration

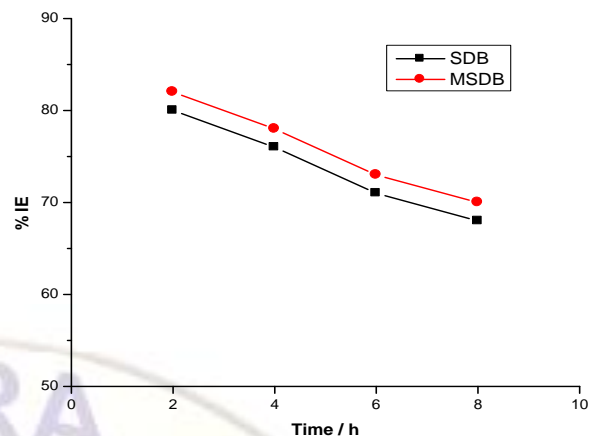
The variation of inhibition efficiency ( $\mu_{WL}\%$ ) with inhibitor concentration is shown in Fig.4(a). Increase in inhibition efficiency at higher concentration of inhibitor may be attributed to larger coverage of metal surface with inhibitor molecules. The maximum inhibition efficiency was achieved at 100 ppm and a further increase in inhibitor concentration caused no appreciable change in performance

#### 3.3.2 Effect of immersion time

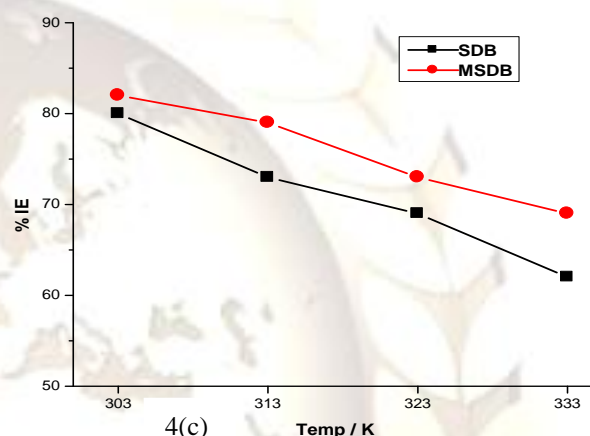
The effect of immersion time on inhibition efficiency is shown in Fig.4(b). All the tested Schiff bases show a decrease in inhibition efficiency with increase in immersion time from 2 to 8 hours. This indicates desorption of the Schiff Base over a longer test period and may be attributed to various other factors such as formation of less persistent film layer on the metal surface, and increase in cathodic reaction or increase in ferrous ion concentration [37].

#### 3.3.3 Effect of temperature

The influence of temperature on inhibition efficiency of two Schiff bases compounds is shown in Fig.4(c). The inhibition efficiency for the two Schiff base compounds decreases with increase in temperature from 303 to 333K. The decrease in inhibition efficiency with rise in temperature may be attributed to desorption of the inhibitor molecules from metal surface at higher temperatures and higher dissolution rates of aluminium at elevated temperatures.

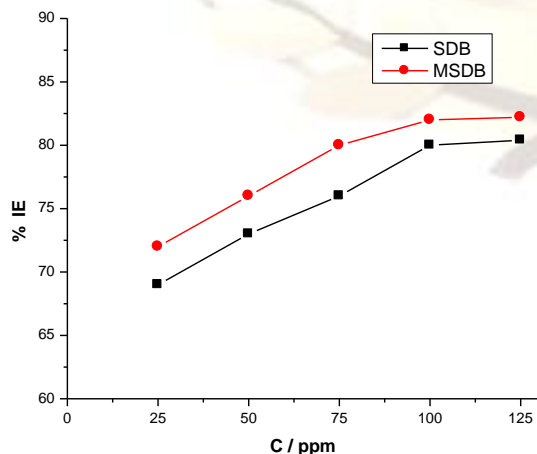


4(b)



4(c)

Figure. 4. Variation of inhibition efficiency with (a) Inhibitor concentration (b) Exposure time (c) Temperature in 1M Hydrochloric acid for SDB and MSDB.



4(a)

Table- 5. Weight loss parameters for AA6063 in 1M hydrochloric acid in the absence and presence of various concentrations of SDB and MSDB at 2 hours of exposure time and different temperature.

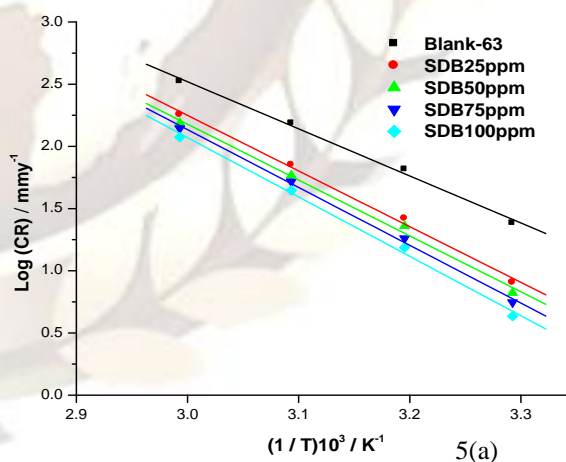
Inhibitor	Conc /ppm	Weight Loss( $\Delta w$ )/ mg, Percentage of Inhibition ( $\mu_{WL}$ %), Corrosion Rate(CR)/ $\text{mmpy}$ , Surface Coverage( $\theta$ )															
		303 K				313 K				323 K				333 K			
		$\Delta w$	$\mu_{WL}$ %	CR	$\theta$	$\Delta w$	$\mu_{WL}$ %	CR	$\theta$	$\Delta w$	$\mu_{WL}$ %	CR	$\theta$	$\Delta w$	$\mu_{WL}$ %	CR	$\theta$
SDB	Blank	13.7	-	21.0	-	49.9	-	76.4	-	102.8	-	157.3	-	199.8	-	305.8	-
	25	4.2	69	6.5	0.69	19.0	62	29.0	0.62	46.3	55	70.8	0.55	101.9	49	155.9	0.49
	50	3.7	73	5.7	0.73	17.5	65	26.7	0.65	42.1	59	64.5	0.59	93.9	53	143.7	0.53
	75	3.3	76	5.0	0.76	16.0	68	24.4	0.68	38.0	63	58.2	0.63	85.9	57	131.5	0.57
	100	2.7	80	4.2	0.80	13.5	73	20.6	0.73	31.9	69	48.8	0.69	75.9	62	116.2	0.62
MSDB	25	3.8	72	5.9	0.72	16.0	68	24.4	0.68	41.1	60	62.9	0.60	93.9	53	143.7	0.53
	50	3.3	76	5.0	0.76	14.0	72	21.4	0.72	37.0	64	56.6	0.64	85.9	57	131.5	0.57
	75	2.7	80	4.2	0.80	12.5	75	19.1	0.75	31.9	69	48.8	0.69	71.9	64	110.1	0.64
	100	2.5	82	3.8	0.82	10.5	79	16.0	0.79	27.8	73	42.5	0.73	61.9	69	94.8	0.69

### 3.3.4 Thermodynamic activation parameters

Thermodynamic activation parameters are important to study the inhibition mechanism. The activation energy ( $E_a$ ) is calculated from the logarithm of the corrosion rate in acidic solution is a linear function of  $(1/T)$  -Arrhenius equation (7):

$$\log(\text{CR}) = -E_a / 2.303RT + A \quad (7)$$

Where,  $E_a$  is the apparent effective activation energy,  $R$  is the universal gas constant and  $A$  is the Arrhenius pre exponential factor. Plots of logarithm of corrosion rate obtained by weight loss measurement versus  $1/T$  gave straight lines and slope equal to  $(-E_a/2.303R)$  as shown in Figs. 5(a) and 5(b) for SDB and MSDB respectively. The  $E_a$  values calculated are listed in Table.6.



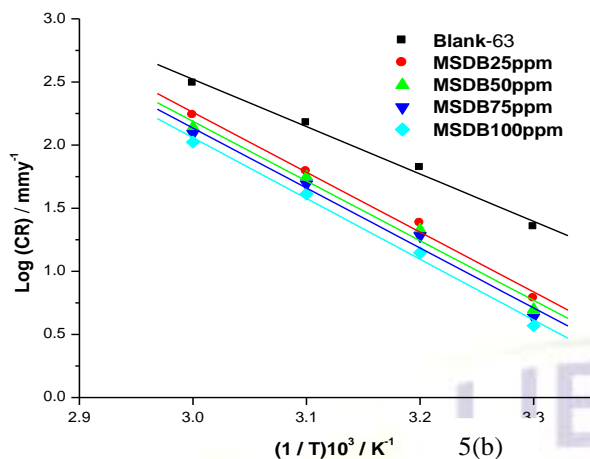


Figure.5. Arrhenius plot of log CR versus 1/T in absence and presence of (a) SDB and (b)MSDB

A plot of log (CR/T) versus 1/T gave a straight line, Figs. 6(a) and (b) with a slope of  $(-\Delta H/2.303 R)$  and an intercept of  $[(\log (R/Nh) + (\Delta S/2.303 R))]$ , from which the values of  $\Delta S^*$  and  $\Delta H^*$  were calculated. The straight lines were obtained according to transition state equation (8):

$$C R = RT / N h \exp(-\Delta H^* / RT) \exp (\Delta S^* / R) \quad (8)$$

Where,  $h$  is the Plank constant,  $N$  is the Avogadro number,  $\Delta S^*$  is entropy of activation and  $\Delta H^*$  is the enthalpy of activation. The  $\Delta S^*$  and  $\Delta H^*$  values calculated are listed in Table. 6

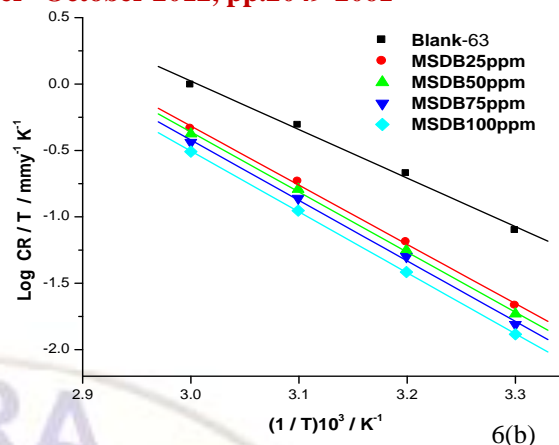
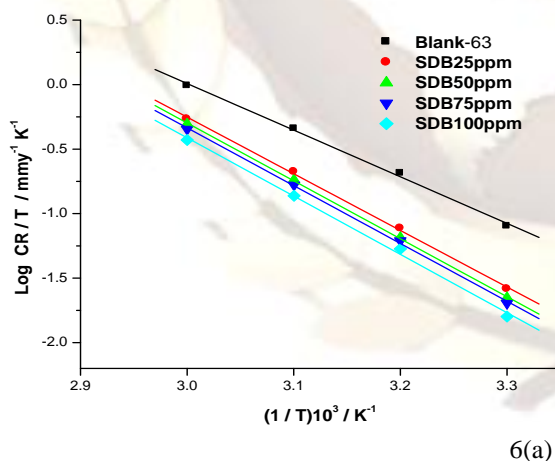


Figure.6. Arrhenius plot of log (CR/T) versus 1/T in absence and presence of (a) SDB and (b) MSDB

Table-6. Thermodynamic parameters of activation of AA6063 in 1M HCl in presence and absence of different concentrations of SDB and MSDB

Table-6. Thermodynamic parameters of activation of AA6063 in 1M HCl in presence and absence of different concentrations of SDB and MSDB

Inhibitor	Concentration (ppm)	$E_a$ (kJmol <sup>-1</sup> )	$\Delta H^*$ (kJmol <sup>-1</sup> )	$\Delta S^*$ (J mol <sup>-1</sup> K <sup>-1</sup> )
SDB	0	72.49	69.22	10.22
	25	85.72	84.08	49.82
	50	86.04	85.97	54.64
	75	89.03	86.00	55.35
	100	91.42	86.55	58.02
MSDB	25	87.06	85.36	52.43
	50	88.77	86.66	55.48
	75	89.92	87.21	55.98
	100	92.16	87.83	56.27

The  $E_a$  values of aluminium alloy in 1M Hydrochloric acid in the presence of Schiff base compounds are higher than those in the absence of Schiff bases. The increase in the  $E_a$  values, with increasing inhibitor concentration is attributed to physical adsorption of inhibitor molecules on the metal surface [38]. In other words, the adsorption of inhibitor on the electrode surface leads to formation of a physical barrier that reduces the metal dissolution in electrochemical reactions [39]. The inhibition efficiency decreases with increase in temperature which indicates desorption of inhibitor molecules as the temperature increases [40]. The values of enthalpy of activation ( $\Delta H^*$ ) are positive; this indicates that the corrosion process is endothermic. The values of entropy of activation ( $\Delta S^*$ ) are higher in the presence of inhibitor than those in the absence of inhibitor, The increase in values of  $\Delta S^*$  reveals that an increase in randomness occurred on going from reactants to the activated complex [41-43].

### 3.3.5 Adsorption isotherms

It is generally assumed that the adsorption of the inhibitor at the interface of metal and solution is the first step in the mechanism of inhibition aggressive media. It is also widely

acknowledged that adsorption isotherms provide useful insights into the mechanism of corrosion inhibition. The investigated compounds inhibit the corrosion by adsorption at the metal surface. Theoretically, the adsorption process has been regarded as a simple substitution adsorption process, in which an organic molecule in the aqueous phase substitutes the water molecules adsorbed on the metal surface [44]. The surface coverage ( $\theta$ ) value calculated from weight loss data for different concentrations of Schiff bases was used to explain the best adsorption isotherm. The value of surface coverage ( $\theta$ ) was tested graphically for fitting a suitable adsorption isotherm. Attempts were made to fit surface coverage ( $\theta$ ) values of various isotherms including Langmuir, Freundlich and Temkin isotherms. Among three adsorption isotherms obtained, the best fitted isotherm was the Langmuir adsorption isotherm ( $C_{(inh)} / \theta$  vs.  $C_{(inh)}$ ) Fig.7(a) with the linear regression coefficient values ( $R^2$ ) in the range of 0.9994 - 0.9996. The Langmuir adsorption isotherm can be expressed by following equation (9):

$$\frac{C_{(inh)}}{\theta} = \frac{1}{K_{(ads)}} + C_{(inh)} \quad (9)$$

Where  $C_{(inh)}$  is inhibitor concentration and  $K_{(ads)}$  is an equilibrium constant for adsorption and desorption.

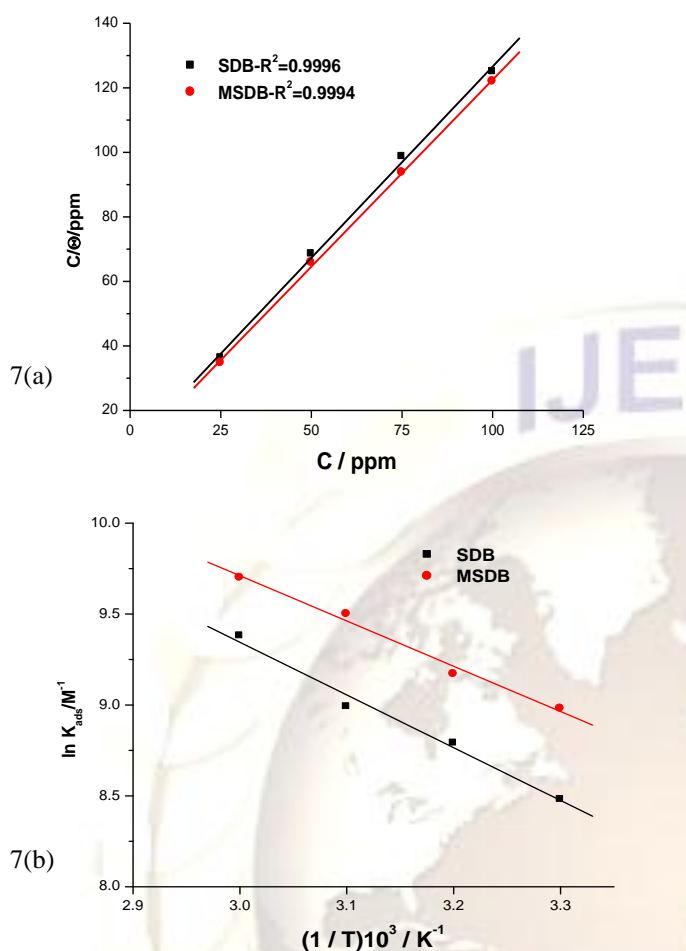
The  $K_{(ads)}$  was calculated from the intercepts of the straight lines on the  $C_{(inh)} / \theta$  axis Fig.7(a) and standard free energy of adsorption of inhibitor  $\Delta G_{ads}^0$  was calculated using the relation (10);

$$\Delta G_{ads}^0 = -RT \ln (55.5 K_{ads}) \quad (10)$$

To calculate heat of adsorption ( $\Delta H_{ads}^0$ ) and entropy of adsorption ( $\Delta S_{ads}^0$ )  $\ln K_{(ads)}$  vs.  $1/T$  was plotted as shown in Fig.7(b). The straight lines were obtained with a slope equal to  $(-\Delta H_{ads}^0 / R)$  and intercept equal to  $(\Delta S_{ads}^0 / R + \ln 1/55.5)$ . The values of equilibrium constant ( $K_{(ads)}$ ), Standard free energy of adsorption ( $\Delta G_{ads}^0$ ), enthalpy of adsorption ( $\Delta H_{ads}^0$ ) and entropy of adsorption ( $\Delta S_{ads}^0$ ) are listed in Table.7.

The negative values of standard free of adsorption indicated spontaneous adsorption of Schiff bases on aluminium alloy surface. The calculated standard free energy of adsorption values for the Schiff bases are closer to  $-40 \text{ kJ mole}^{-1}$  and it can be concluded that the adsorption of Schiff bases on the aluminium surface is more chemical than physical one [45]. The sign of enthalpy and entropy of adsorption are positive and is related to substitutional adsorption can be attributed to the increase in the solvent entropy and to a more positive water desorption enthalpy. The increase in entropy is the driving force for the adsorption of the Schiff bases on the aluminium alloy surface.

The adsorption of Schiff base on the aluminium alloy surface can be attributed to adsorption of the organic compounds via phenolic and iminic groups in both cases. Among these two Schiff bases, the chelate effect of MSDB is greater than that of SDB. This is due to the presence of two electron donating groups of  $-\text{OCH}_3$  in MSDB structure than SDB. The more efficient adsorption of MSDB is the result of electronegative oxygen atoms present in the MSDB compared to SDB Structure.



Inhibitor	Concentration (ppm)	Temperature (K)	$K_{ads}$ ( $10^3 M^{-1}$ )	$\Delta G_{ads}^{\circ}$ (kJmol $^{-1}$ )	$\Delta H_{ads}^{\circ}$ (kJmol $^{-1}$ )	$\Delta S_{ads}^{\circ}$ (Jmol $^{-1}$ )
SDB	100	303	11.94	-34	24.1	183
		313	8.01	-34		
		323	6.60	-34		
		333	4.84	-35		
MSDB	100	303	16.2	-35	20.7	176
		313	13.4	-35		
		323	9.64	-35		
		333	7.93	-36		

Table-7. Thermodynamic parameters for the adsorption of inhibitor in 1M HCl on AA6063 alloy at different temperatures

Figure.7. (a) Langmuir adsorption isotherm plot and (b) Heat of adsorption isotherm plot for SDB and MSDB

### 3.4 Scanning electron microscope (SEM)

Scanning electron microscopy of the AA6063 sample of inhibited and uninhibited metal samples is presented in Fig. 8. The SEM study shows that the inhibited alloy surface is found smoother than the uninhibited surface.

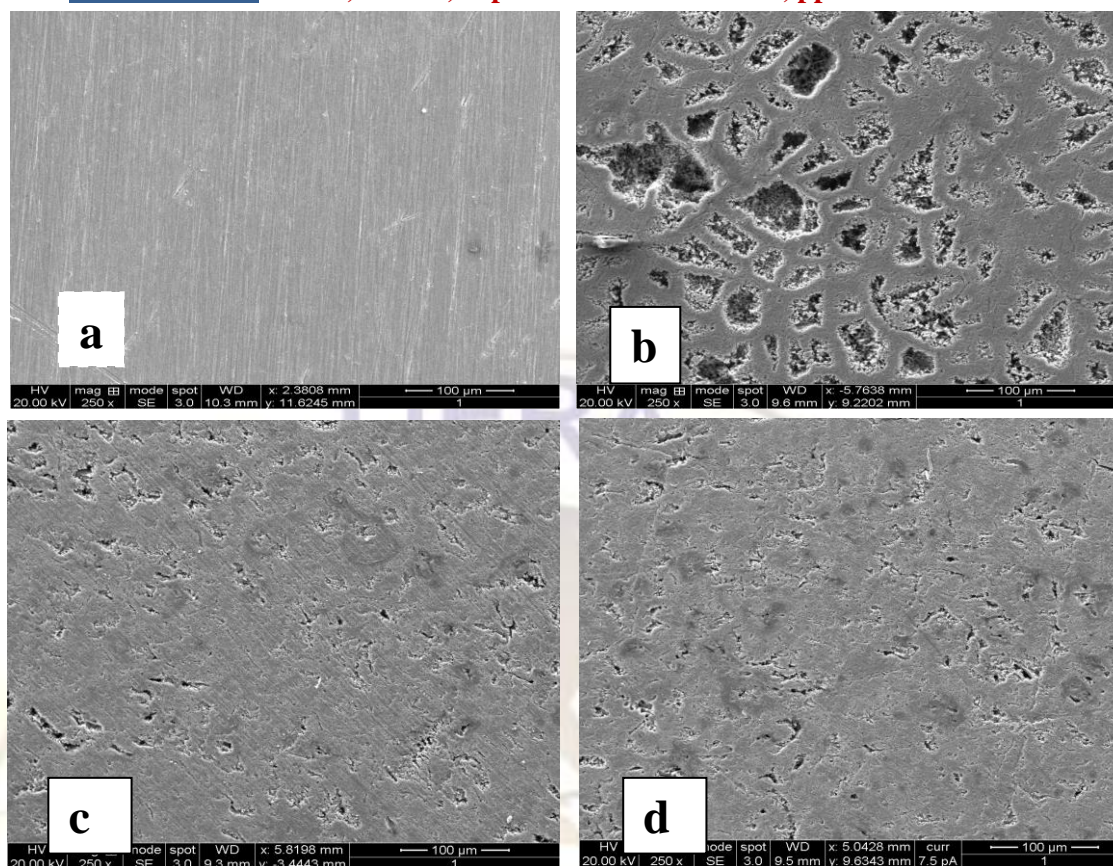


Figure. 8. Scanning electron micrographs of (a) Polished AA6063 alloy, (b) After immersion in 1M HCl for 2h, (c) After immersion in 1M HCl for 2h in presence of 100 ppm SDB and (d) After immersion in 1M HCl for 2h in presence of 100 ppm MSDB.

#### 4. Conclusions

1. The investigated Schiff bases are good inhibitors for aluminium alloy 6063 in 1M Hydrochloric acid solution.
2. In weight loss studies, the inhibition efficiency ( $\mu_{WL}\%$ ) of the Schiff bases increase with increase in inhibitor concentration, whereas decreases with increase in immersion time and temperature.
3. Potentiodynamic polarisation studies demonstrate the Schiff bases under investigation act as mixed type but predominantly cathodic inhibitors.
4. EIS measurements show that as the inhibitor concentration is increased, the charge transfer resistance increases and double layer capacitance decreases.
5. The inhibition efficiency obtained using weight loss, potentiodynamic polarisation, and EIS studies are in good agreement and in accordance to the order: MSDB > SDB for AA6063.
6. The adsorptions of Schiff bases on alloy surface in 1M HCl solution are governed by Langmuir adsorption isotherm.

7. Scanning Electron Microscopy (SEM) shows a smoother surface for inhibited alloy samples than uninhibited samples due to formation of protective barrier film.

#### References:

1. U.Ergun, D.Yuzer and K.C.Emregul, *Mater. Chem.Phys.*, 109(2008)492-499.
2. T.Hurlen, H.H.Lian, O.S.Odegard and T.V.Valand *Mater.Chem.Phys.*,29(1984)579-585.
3. A.K.Maayta, N.A.F.Al-Rawashdeh, *Corros.Sci.* 46 (2004) 1129.
4. E.E.Oguzie, *Mater.Lett.* 59 (2005) 1076.
5. A. Popova, M. Chouristov, S. Raicheva, E. Sokolova, *Corros. Sci.* 46 (2004) 1333.
6. R.G. Nuzzo, E.M. Korenic, L.H. Dubois, *J. Chem. Phys.* 93, 767 (1980).
7. A.Aytac, U.Ozmen and M.Kabbasakaloglu, *Mater.Chem.Phys.*, 89(2005)176.
8. Hahner, G., Woll, Ch., Buck, M., Grunze, M., 1993. *Langmuir* 9 (1), 955.

9. H. Shorky, M. Yuasa, I. Sekine, R.M. Issa, H.Y. El-Baradie, G.K. Gomma, *Corros. Sci.* 40, 2173 (1998).
10. C.D. Bain, E.B. Thouroughton, Y.T. Tao, J. Evall, G.M. Whiteside, J.G. Nuzzo, *J. Am. Soc.* 111, 321.
11. Z. Quan, S.H. Chen, Y. Li, X. Cui, *Corros. Sci.* 44, 703 (2002).
12. S.L. Li, Y.G. Wang, S.H. Chen, R. Yu, S.B. Lei, H.Y. Ma, D.X. Liu, *Corros. Sci.* 41, 1769 (1999).
13. Ashish Kumar Singh, M. A. Quraishi, *Int. J. Electrochem. Sci.*, 7 (2012) 3222-3241.
14. Fatemeh baghaei Ravari, Athareh Dadagarinezhad, Iran Shekhshoei, *J. Chi. Chem. Soc.* 55, N° 3 (2010) 328-331.
15. Fatemeh baghaei Ravari, Athareh Dadagarinezhad, Iran Shekhshoei, *G.U. Journal of Science.* 22(3);175-182 (2009).
16. A.S. Patel, V. A. Panchal, G. V. Mudaliar, N. K. Singh, *Journal of Saudi Chemical society* (2011)xxx, xxx, xxx.
17. A. S. Patel, V. A. Panchal and N. K. Shah, *PRAJÑĀ - Journal of Pure and Applied Sciences, Vol. 18: 73 - 75* (2010).
18. T. Sethi, A. Chaturvedi, R. K. Upadhyaya, and S. P. Mathur, *Protection of Metals and Physical Chemistry of Surfaces*, 2009, Vol. 45, No. 4, pp. 466-471.
19. A. S. FOU DA, G. Y. ELEWADY, A. EL-ASKALANY, K. SHALABI, *ZASTITA MATERI JALA 51* (2010) broj 4, Scientific paper UDC:620.197.3:669.717
20. John Reglinski , Samantha Morris, Davina E. Stevenson *Polyhedron 21* (2002) 2175-2182 .
21. ASTM (2004) Standard practice for Laboratory Immersion Corrosion Testing of Metals G31-72.
22. A. Yurt, S. Ulutas, H. Dal, *Appl. Surf. Sci.* 253 (2006) 919.
23. A. El-Sayed, *Corros. Prev. Control* 43 (1996) 23.).
24. M. Metikos-Hukovic, R. Babic, Z. Grubac, *J. Appl. Electrochem.* 28 (1998) 433.
25. C.M.A. Brett, *J. Appl. Electrochem.* 20 (1990) 1000.
26. E.J. Lee, S.I. Pyun, *Corros. Sci.* 37 (1995) 157.
27. C.M.A. Brett, *Corros. Sci.* 33 (1992) 203.
28. K.F. Khaled, M.M. Al-Qahtani, *Mater. Chem. Phys.* 113 (2009) 150.
29. A. Ehteram Noor, *Mater. Chem. Phys.* 114 (2009) 533.
30. A. Aytac, U. Ozmen, M. Kabasakaloglu, *Mater. Chem. Phys.* 89 (2005) 176.
31. T. Pajkossy, *J. Electroanal. Chem.* 364, 111, (1994).
32. W.R. Fawcett, Z. Kovacova, A. Mtheo, C. Foss, *J. Electroanal. Chem.* 326, 91, (1992).
33. R. deLevi, *Electrochem. Acta* 8 (1963) 751.
34. H.J.W. Lenderink, M.V.D. Linden, J.H.W. De Wit, *Electrochim. Acta* 38 (1989) 1993.)
35. F. Mansfeld, C.H. Tsai, H. Shih, in: R.S. Munn (Ed.), *Computer Modeling in Corrosion, ASTM, Philadelphia, PA, 1992*, p. 86.
36. C.H. Hsu, F. Mansfeld, *corrosion* 57 (2001) 747.
37. M.A Quraishi. *Rawat J (2001) Corrosion* 19: 273.
38. H. Ashassi-Sorkhabi, B. Shaabani, D. Seifzadeh, *Appl. Surf. Sci.* 239 (2005) 154.
39. F. Mansfeld, *Corrosion Mechanism*, Marcel Dekkar, New York, 1987, p. 119.
40. Ashish Kumar Singh, M.A. Quraishi, *Corros. Sci.* 52 (2010) 156.
41. E.A. Noor, A.H. Al-Moubaraki, *Mater. Chem. Phys.* 110 (2008) 145.
42. A. Yurt, A. Balaban, S.U. Kandemir, G. Bereket, B. Erk, *Mater. Chem. Phys.* 85(2004) 420.
43. G.E. Badr, *Corros. Sci.* (2009), doi:10.1016/j.corosci.2009.06.017.
44. T. Paskossy, *J. Electroanal. Chem.* 364 (1994) 111.
45. A.Yurt, A. Balaban. S. Ustin Kandemir, G. Bereket. B. Erk, *Mateerials Chemistry and physics.* 85 (2004) 420-426.

#### **Acknowledgement**

Authors would like to thank for their encouragement to Dr. M.A. Quraishi, Professor of Chemistry, Banaras Hindu University (BHU), Varanasi, India, Dr. D.B. Fakruddin, Professor Emeritus, Siddaganga Institute of Technology, Tumkur, India, Thanks are due to Dr. Syed Abu Sayeed Mohammed, Prof. MN Zulfiqar Ahmed and Mr. Syed Nayazulla of department of Engineering Chemistry, Ms. Soni. M. EEE department, HKBK College of Engineering, for their contribut